



# A statistical study of C IV regions in 20 Oe-stars

A. Antoniou<sup>a,\*</sup>, E. Danezis<sup>a</sup>, E. Lyratzi<sup>a,b</sup>, L.Č. Popović<sup>c</sup>, D. Stathopoulos<sup>a</sup>,  
M.S. Dimitrijević<sup>c</sup>

<sup>a</sup> University of Athens, Faculty of Physics, Department of Astrophysics, Astronomy and Mechanics, Panepistimioupoli, Zographou, 157 84 Athens, Greece

<sup>b</sup> Eugenides Foundation, 387 Sygrou Av., 17564 Athens, Greece

<sup>c</sup> Astronomical Observatory of Belgrade, Volgina 7, 11160 Belgrade, Serbia

Available online 3 February 2014

## Abstract

In this paper, using the Gauss-Rotation model (GR model), we analyse the UV C IV resonance lines in the spectra of 20 Oe-stars of different spectral subtypes, in order to detect the structure of C IV region. We study the presence and behavior of absorption clouds and analyse their characteristics. From this analysis we can calculate the values of a group of physical parameters, such as the apparent rotational and radial velocities, the random velocities of the thermal motions of the ions, the Full Width at Half Maximum (FWHM), the optical depth, as well as the absorbed energy and the column density of the independent regions of matter, which produce the main and the satellite clouds of the studied spectral lines. Finally, we present the relations between these physical parameters and the spectral subtypes of the studied stars and we give our results about the structure of the C IV region in their atmosphere.

© 2014 COSPAR. Published by Elsevier Ltd. All rights reserved.

**Keywords:** Oe stars; C IV resonance lines; Density clouds; Rotational velocities; Radial velocities; Random velocities

## 1. Introduction

The C IV resonance lines in the Oe stellar spectra have a peculiar and complex profile. Additionally many researchers have observed the existence of absorption C IV components shifted to the violet side of the main spectral line e.g. Doazan et al. (1991), Danezis et al. (1991,2003) [p. 180], Danezis et al. (2007) [p. 828] and Lyratzi et al. (2007) [p. 358]. We named these components Discrete or Satellite Absorption Components (DACs: Bates and Halliwell, 1986 [p. 678] SACs: Danezis et al., 2003[p. 180]). DACs or SACs originate in separate density clouds, in the C IV region and have different rotational and radial velocities. In any case, the whole observed feature of the C IV

resonance lines is not the result of a uniform atmospherical region, but it results from different CIV clouds with different physical parameters, which create a series of components. This analysis improves and completes our preliminary previous work (Antoniou et al., 2007). Using the Gauss-Rotation Model (GR model) (Danezis et al., 2007), we analyse the UV C IV ( $\lambda\lambda$  1548.155 Å, 1550.774 Å) resonance lines in the spectra of 20 Oe-stars of different spectral subtypes, taken with IUE, in order to investigate the presence of Satellite Absorption Components (SACs) and Discrete Absorptions Components (DACs). From this analysis we can calculate the values of a group of physical parameters, such as the apparent rotational and radial velocities of the density clouds, the random velocities of the thermal motions of the ions, the Full Width at Half Maximum (FWHM), the optical depth, as well as the absorbed energy and the column density of the independent C IV clouds of matter, which produce the main and the satellites components of the studied spectral lines. The knowledge of these parameters allows us to

\* Corresponding author. Tel.: +306974827592.

E-mail addresses: [ananton@phys.uoa.gr](mailto:ananton@phys.uoa.gr) (A. Antoniou), [edanezis@phys.uoa.gr](mailto:edanezis@phys.uoa.gr) (E. Danezis), [elyratzi@phys.uoa.gr](mailto:elyratzi@phys.uoa.gr) (E. Lyratzi), [ipopovic@aob.bg.ac.rs](mailto:ipopovic@aob.bg.ac.rs) (L.Č. Popović), [dstatho@phys.uoa.gr](mailto:dstatho@phys.uoa.gr) (D. Stathopoulos), [mdimitrijevic@aob.rs](mailto:mdimitrijevic@aob.rs) (M.S. Dimitrijević).

Table 1

The twenty studied stars with their spectral subtype and effective temperature

Star	Spectral Subtype	Name	Teff (kK)
HD24534	O9.5 III	X Per	32
HD24912	O7.5 III ((f))	ξ/46 Per	36
HD34656	O7 II (f)	–	36.8
HD36486	O9.5 II	δ/34 Ori	33.5
HD37022	O6 Vp	θ Ori	45.5
HD47129	O7.5 III	V640 Mon	35
HD47839	O7 III	15/S Mon	41
HD48099	O6.5 V	–	39
HD49798	O6p	–	47
HD57060	O8.5If	29/UW CMa	35.9
HD57061	O9.0I	τ /30 CMa	31.8
HD60848	O8.0Vpe	BN Gem	36.5
HD91824	O7V ((f))	–	39
HD93521	O9.5II	–	34
HD112244	O8.5Iab	–	32
HD149757	O9V (e)	ζ Oph	34
HD164794	O4V ((f))	9 Sgr	46
HD203064	O8V	68 Cyg	36
HD209975	O9.5I	19 Cep	30.2
HD210839	O6.0I	λ/22 Cep	38

understand the structure of the regions, where the C IV spectral lines are created. Finally, we present the variation of them as a function of the stars' effective temperatures. It is known that the star's effective temperature is related to its spectral subtype. This means that the variation of the parameters as a function of the effective temperature is equivalent to the variation of them as a function of the spectral subtype. In some cases we calculate the linear regression and the linear correlation coefficient  $R^2$ . At the

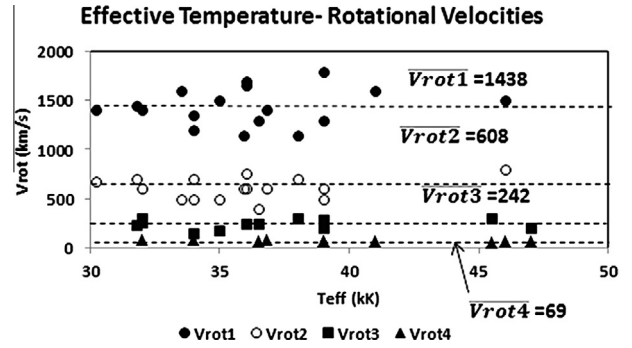


Fig. 2. Variation of the rotational velocities of the C IV resonance lines ( $\lambda\lambda$  1548.155, 1550.774 Å) for the independent density clouds which create the absorption components, as a function of the effective temperature. We have calculated four levels of rotational velocities with mean values 1438, 608, 242 and 69 km/s respectively.

end of the paper we give, as appendices, a short description of the GR model, the linear regression and the linear correlation coefficient.

## 2. Data

The spectrograms of the 20 Oe-stars have been taken with IUE satellite, with the Short Wavelength range Prime and Redundant cameras (SWP, SWR) at high resolution (0.1–0.3 Å). Our sample includes the subtypes O4 (one star), O6 (four stars), O7 (five stars) O8 (three stars) and O9 (seven stars). In Table 1 one can see the studied stars, the spectral subtype and the effective temperature of the studied stars. The best fit has been obtained with two

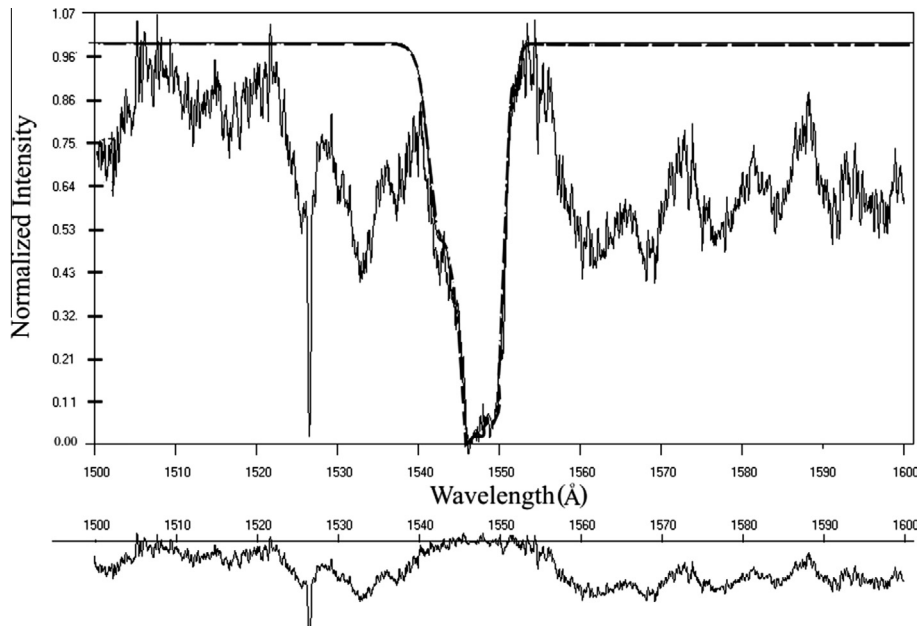


Fig. 1. The C IV doublet of the O9.5 II star HD 93521 and its best fit. The best fit has been obtained using four absorption components. The graph below the profile indicates the difference between the fit from GR model and the real spectral line. The smaller this difference is, the better the quality of fitting. The axis of the graph below corresponds to the wavelength and has the same units (Å) and the same scale as the axis above.

components in nine of the twenty studied stars, with three components in six of them and with four components in five of them.

### 3. Variation of the physical parameters of the C IV regions, as a function of the effective temperature

In Fig. 1 one can see the C IV doublet of the O9.5 II star HD 93521 and its best fit. The best fit has been obtained using four absorption components. The graph below the profile indicates the difference between the fit and the real spectral line.

In the following figures one can see the variation of the physical parameters of the C IV regions of the studied stars, as a function of the stars' effective temperature ( $T_{\text{eff}}$ ). In some cases we give the linear regression and the respective linear correlation coefficient  $R^2$  (see Appendix B and Kleinbaum et al., 1987).

In Fig. 2 we present the variation of the rotational velocities of the C IV resonance lines ( $\lambda\lambda$  1548.155, 1550.774 Å) for the independent density regions of matter, which create the absorption components, as a function of the effective temperature. With the term “rotational velocities” we mean the self rotation of the absorbing clouds. This means that these velocities originate from regions outside the star and not from the star's rotation. We found four groups of rotational velocities. One can observe that we have calculated high values of rotational velocities, especially for the first and second group (mean values 1438 and 608 km/s respectively). An important phenomenon that can be detected in the spectra of hot emission stars is that in many spectra some of these components of highly ionized species are very broad. This very large width cannot be explained as if it is due to large velocities of random

motions of the ions, nor to large rotational velocities of the regions where these components are created. Danezis et al. (2009) have given a possible explanation of this phenomenon. In the environment of hot emission stars, apart from the density regions, the violent mass ejection may produce smaller regions due to micro-turbulent movements. These smaller regions produce narrow absorption components with different shifts that create a sequence of lines. The synthesis of all the lines of this sequence gives us the sense of line broadening. As a result, what we measure as very broad absorption line, is the composition of the narrow absorption lines that are created by micro-turbulent effects. In Fig. 3, in (a)–(c) one can see how a sequence of lines could produce an apparent very broad absorption spectral line. This means that when the width of each of the narrow lines is increasing (from a to c), the final observed feature looks like a single very broad absorption spectral line. In (d) one can see a combination of the apparent very broad absorption spectral line with a classical absorption line. We note that with the term “classical absorption line” we mean the spectral line which has such a profile that can be fitted with a classical mathematical distribution, such as a Gauss, Lorentz (Cauchy) or Voigt distribution.

We applied this idea in some stars and we present the results in the case of the star HD 24912. In Fig. 4 we see the 1st absorption component of the C IV resonance line ( $\lambda$ 1548.155 Å) of the star HD 24912. It corresponds to a rotational velocity of 1700 km/s. According to the previous mentioned idea, it is produced by narrow absorption components with different shifts and different rotational velocities. In this case we obtained the best fit using four components with rotational velocities of 300, 400, 450 and 400 km/s. These components are shown separately below.

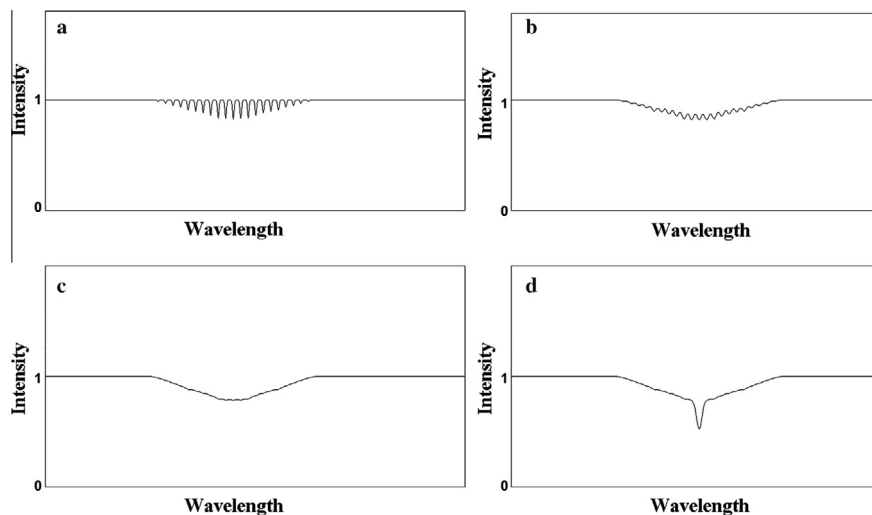


Fig. 3. The addition of all the lines of this sequence gives us the sense of line broadening. As a result, what we measure as very broad absorption line, is the composition of the narrow absorption lines that are created by micro-turbulent effects. This means that when the width of each of the narrow lines is increasing (from a to c), the final observed feature looks like a single very broad absorption spectral line. In (d) one can see a combination of the apparent very broad absorption spectral line with a classical absorption line. We remind that a classical absorption line is a spectral line which has such a profile that can be fitted with a classical mathematical distribution, such as a Gauss, Lorentz (Cauchy) or Voigt distribution.

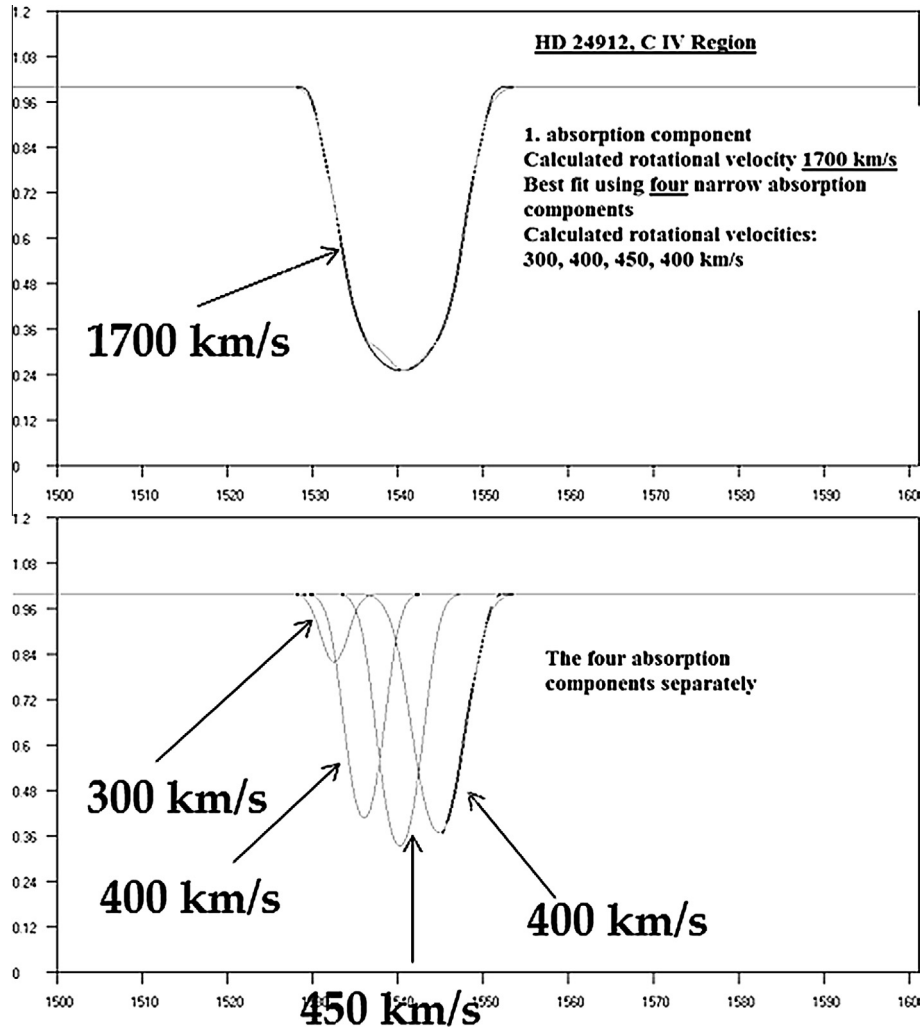


Fig. 4. The first absorption component of the C IV resonance line ( $\lambda$  1548.155 Å) of the star HD 24912. It corresponds to a rotational velocity of 1700 km/s. It is produced by narrow absorption components with different shifts and different rotational velocities. In this case we obtained the best fit using four components with rotational velocities of 300, 400, 450 and 400 km/s. These components are shown separately below.

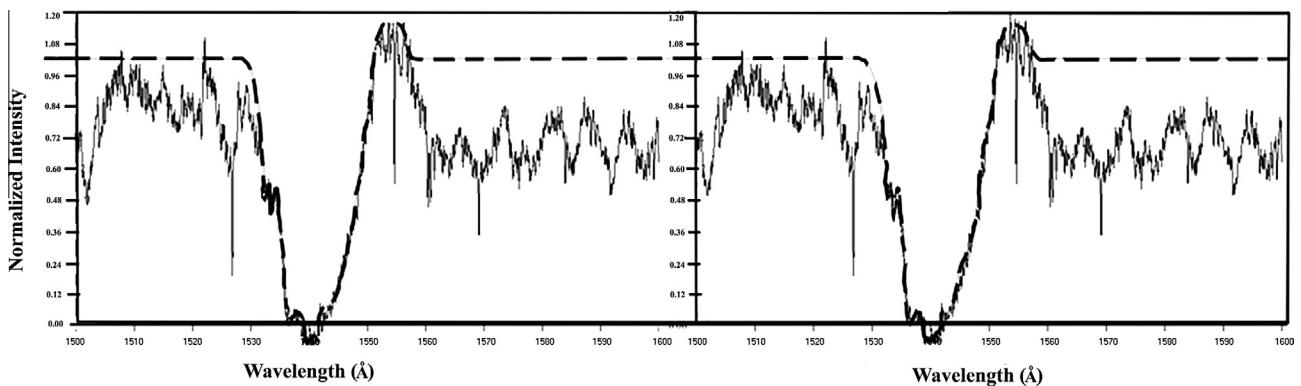


Fig. 5. The best fit using the broad absorption component which corresponds to the rotational velocity of 1700 km/s (left) and the best fit using the four narrow absorption components with different shifts and different rotational velocities with values 300, 400, 450 and 400 km/s (right).

In Fig. 5 one can see the best fit using the broad absorption component, which corresponds to the rotational velocity of 1700 km/s (left) and the best fit using the four

absorption components with different shifts and different rotational velocities with values 300, 400, 450 and 400 km/s (right). The F-test shows as suitable best fit the

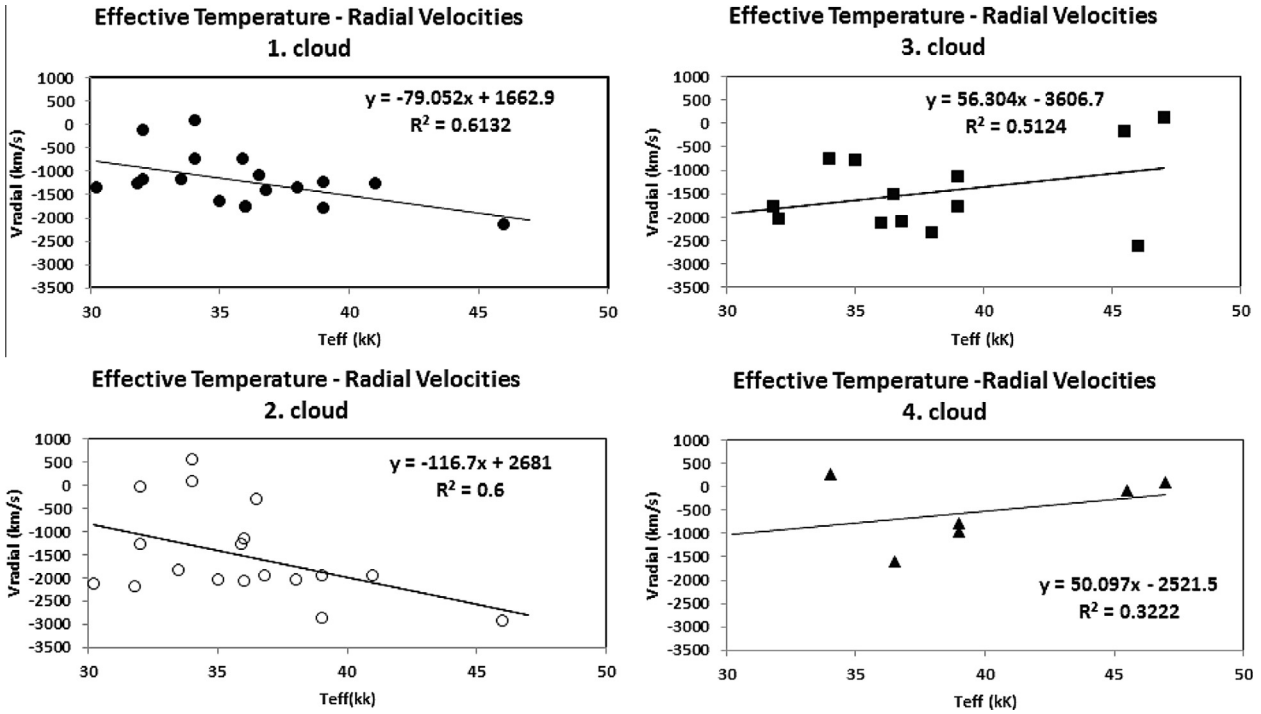


Fig. 6. The variation of the radial velocities of the C IV resonance lines ( $\lambda\lambda$  1548.155, 1550.774 Å) for the independent density regions of matter which create the absorption components, as a function of the effective temperature.

left one. We use the F-test (e.g. [Snedecor and Cochran, 1989](#), Ch. 6, p. 222) in order to check if the fit of a group of (n + 1) absorption components is better from a group of (n) absorption components. This statistical method allows us to choose the minimum number of the absorption components which give the best fit of the particular and

complex spectral lines, which appear in the UV spectra of the hot emission stars (Oe and Be stars).

In [Fig. 6](#) we present the variation of the radial velocities of the C IV resonance lines ( $\lambda\lambda$  1548.155, 1550.774 Å) for the independent density regions of matter, which create the absorption components, as a function of the effective

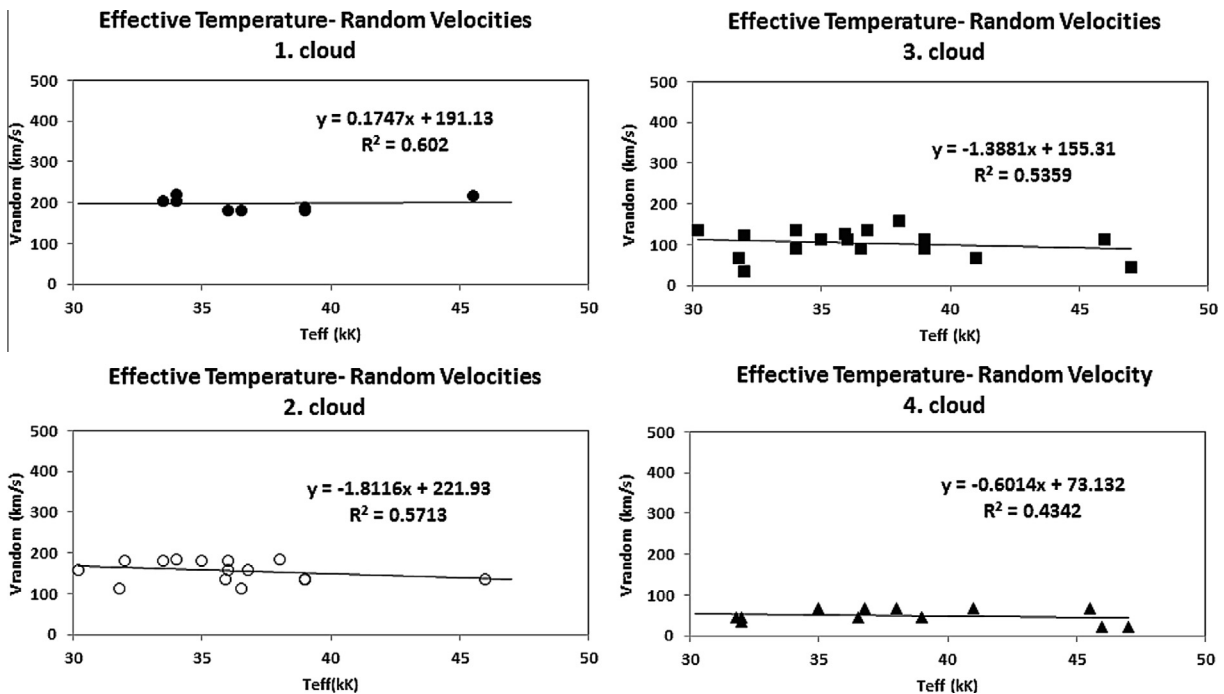


Fig. 7. The variation of the random velocities of the C IV resonance lines ( $\lambda\lambda$  1548.155, 1550.774 Å) for the independent density regions of matter which create the absorption components, as a function of the effective temperature.

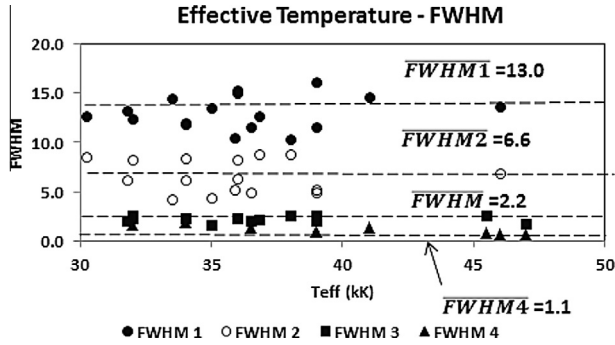


Fig. 8. The variation of the FWHM of the C IV resonance lines ( $\lambda\lambda$  1548.155, 1550.774 Å) for the independent density regions of matter, which create the absorption components, as a function of the effective temperature.

temperature. For the 1st and 2nd cloud we found a slightly negative slope and for the 3rd and 4th cloud a slightly positive slope. We calculated “good” linear correlation for the three components ( $R^2 = 0.6132, 0.6, 0.5124$ ) and “weak” linear correlation for the 4th one ( $R^2 = 0.3222$ ).

In Fig. 7 one can see the variation of the random velocities of the ions of the C IV resonance lines ( $\lambda\lambda$  1548.155, 1550.774 Å) for the independent density regions of matter which create the absorption components, as a function of the effective temperature. We detected an almost constant trend of the random velocities with values between 120 and 200 km/s for the three first clouds and about 80 km/s for the fourth one. The linear correlation is “good”.

The variation of the FWHM is the same as the variation of the rotational and random velocities. This is expected because the FWHM is a parameter which indicates the line broadening and the rotational and random velocities are parameters which contribute to this situation. The average values of the FWHM are 13.0, 6.6, 2.2 and 1.1 Å, respectively. The mentioned can be seen in Fig. 8.

In Figs. 9 and 10 we present the variation of the optical depth ( $\xi$ ) in the C IV resonance lines ( $\lambda\lambda$  1548.155, 1550.774 Å) respectively. The variation of the optical depth presents an almost constant behavior in both of the C IV resonance lines. The optical depth’s values in the C IV ( $\lambda$  1550.774 Å) spectral line are 0.9 of the optical depth’s values in the C IV ( $\lambda$  1548.155) Å. This is in agreement with the atomic theory because, according to this theory, the laboratory intensity ratio of the two C IV resonance spectral lines is also 0.9.

In Figs. 11 and 12 one can see the variation of the absorbed energy ( $E_a$ ) in the C IV resonance lines ( $\lambda\lambda$  1548.155, 1550.774 Å) respectively. The absorbed energy of a density cloud, which is in the optical line of the observer, is the part of the “black body star” radiation which is absorbed from a specific density cloud. The variation of the absorbed energy, as in the case of the optical depth, presents almost the same behavior in both of the C IV resonance lines and the ratio 0.9 between the two C IV resonance lines is maintained. This is expected because the absorbed energy is an index of the optical depth.

Finally, in Figs. 13 and 14 one can see the variation of the column density (CD) in the C IV resonance lines  $\lambda\lambda$

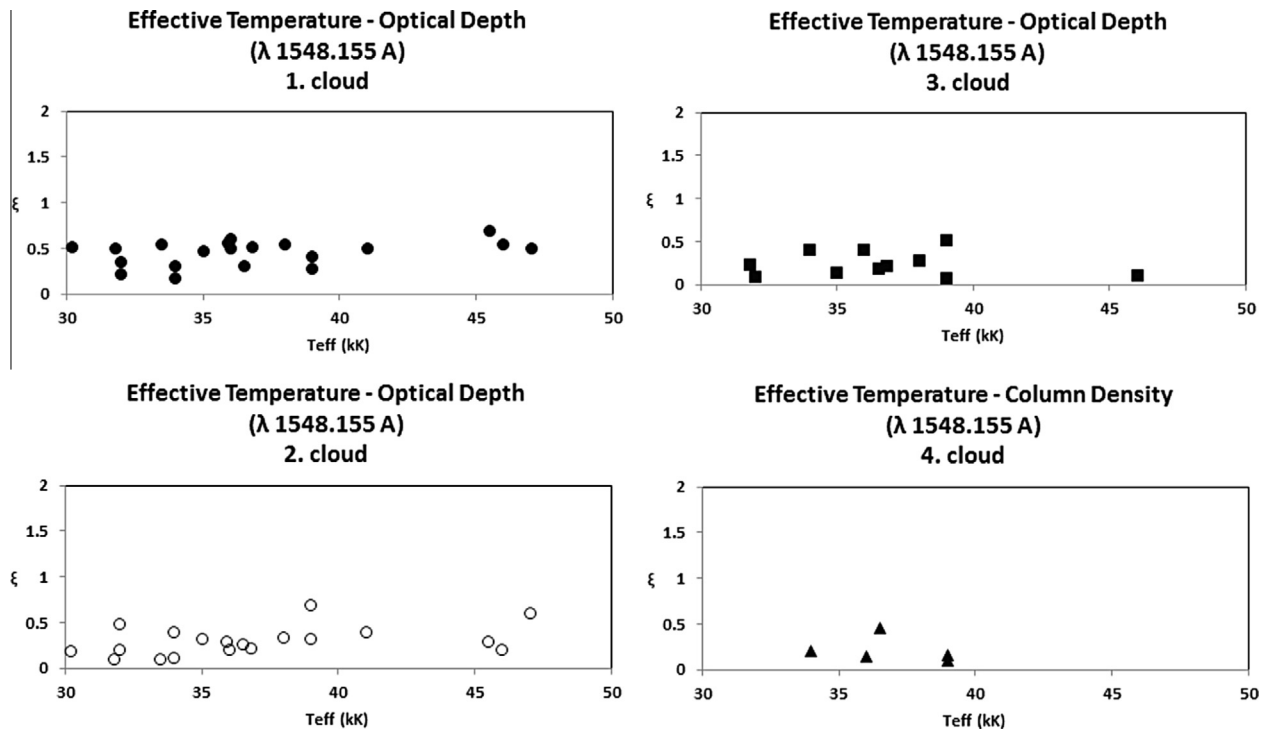


Fig. 9. The variation of the optical depth ( $\xi$ ) of the C IV resonance line ( $\lambda\lambda$  1548.155 Å) for the independent density regions of matter, which create the absorption components, as a function of the effective temperature.

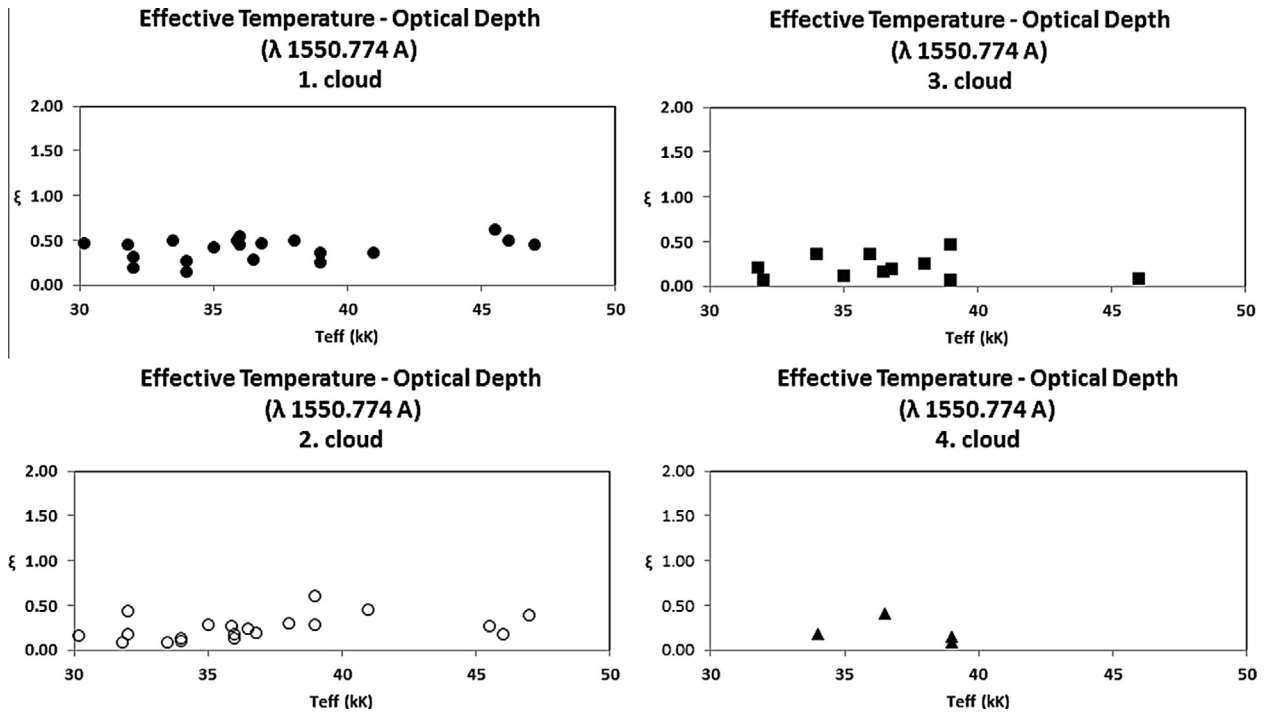


Fig. 10. The variation of the optical depth ( $\xi$ ) of the C IV resonance line ( $\lambda\lambda$  1550.774 Å) for the independent density regions of matter, which create the absorption components, as a function of the effective temperature.

1548.155, 1550.774 Å respectively. The variation of the column density of the C IV resonance lines ( $\lambda\lambda$  1548.155, 1550.774 Å) remains almost constant between  $1 \times 10^{10}$  and  $4 \times 10^{10} \text{ cm}^{-2}$ .

#### 4. Discussion and conclusions

At first we note that the values of all the calculated parameters are included in the acceptable limits of the

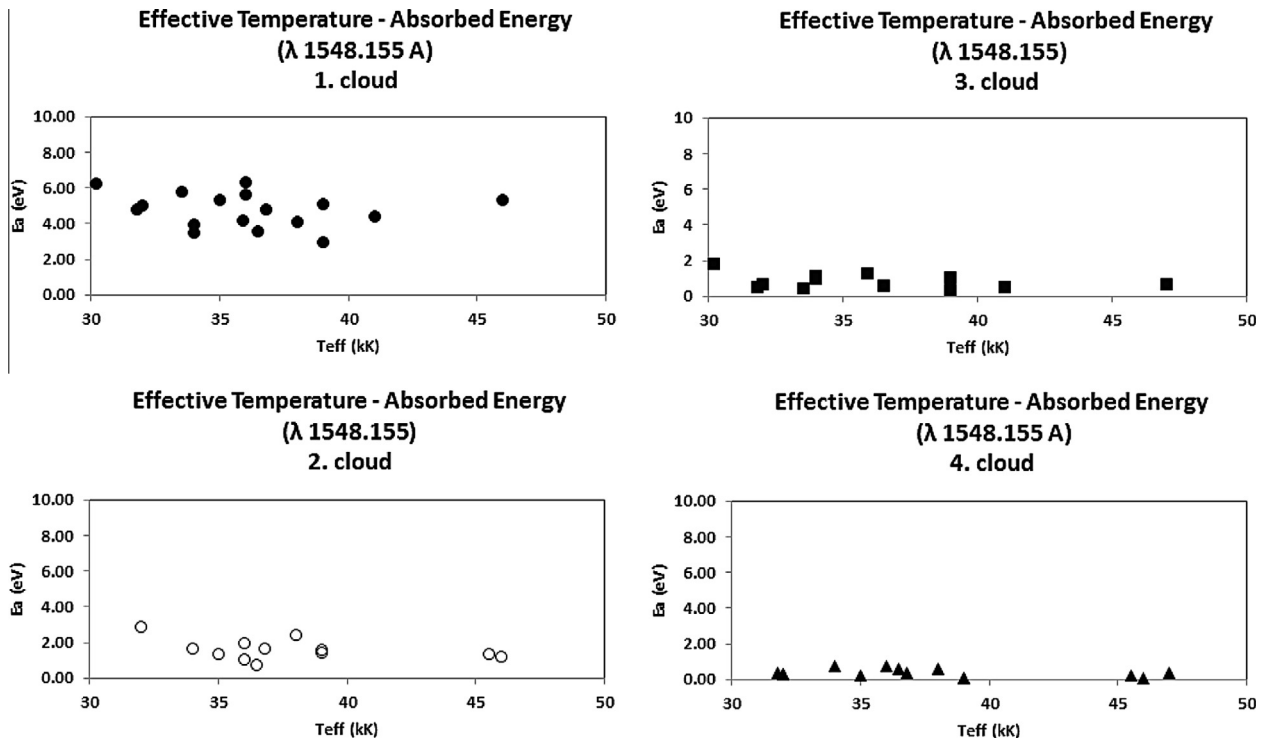


Fig. 11. The variation of the absorbed energy ( $E_a$ ) of the C IV resonance line  $\lambda$  1548.155 Å, for the independent density regions of matter, which create the absorption components, as a function of the effective temperature.

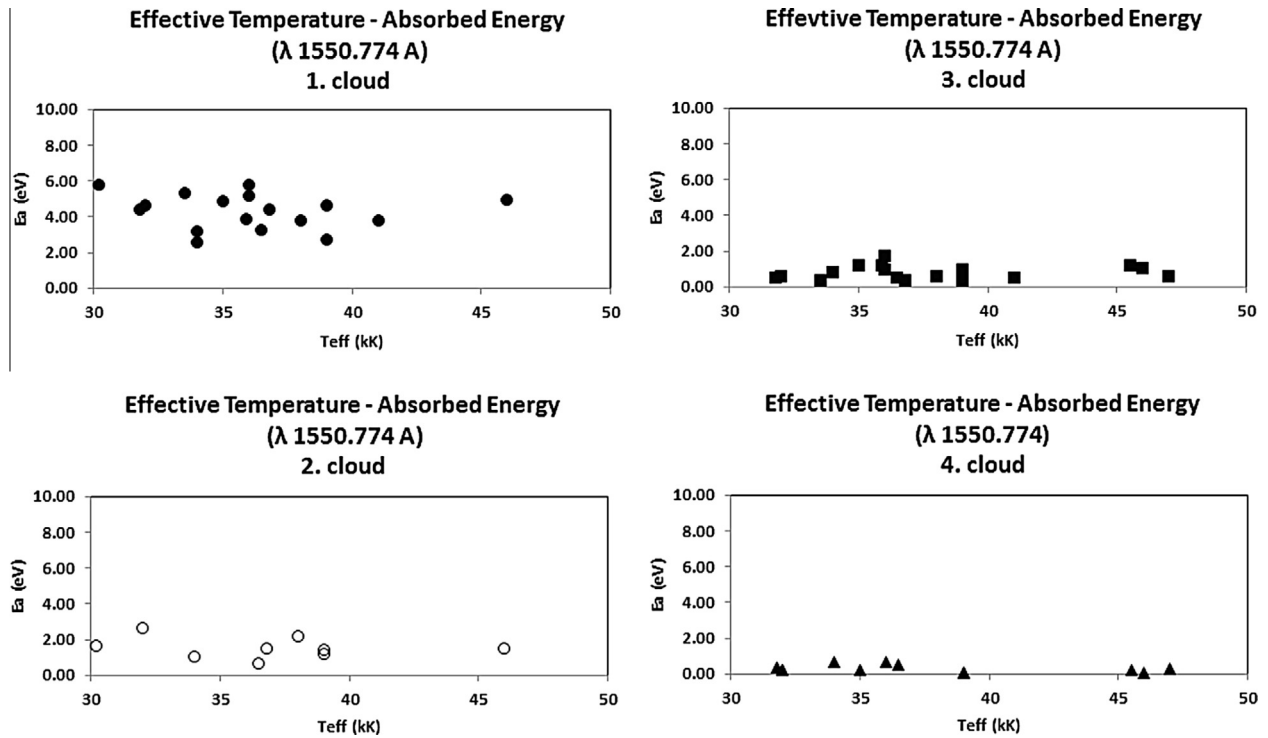


Fig. 12. The variation of the absorbed energy ( $E_a$ ) of the C IV resonance line  $\lambda 1550.774 \text{ \AA}$ , for the independent density regions of matter, which create the absorption components, as a function of the effective temperature.

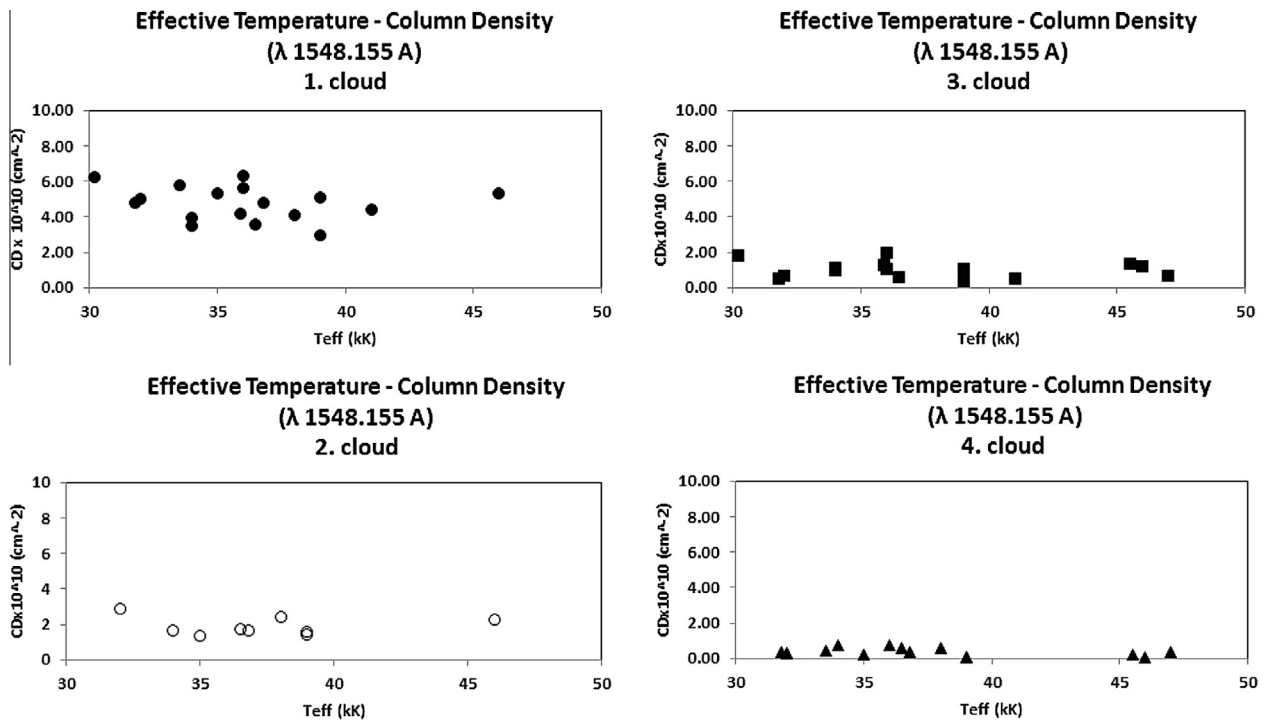


Fig. 13. The variation of the column density (CD) of the C IV resonance line  $\lambda 1548.155 \text{ \AA}$ , for the independent density regions of matter, which create the absorption components, as a function of the effective temperature.

theory of the hot emission stars’ atmospheric structure. With regard to the calculated parameters, we remark the following:

*Rotational velocities*

We have detected four groups of the rotational velocities’ values. One can distinguish these groups as describing

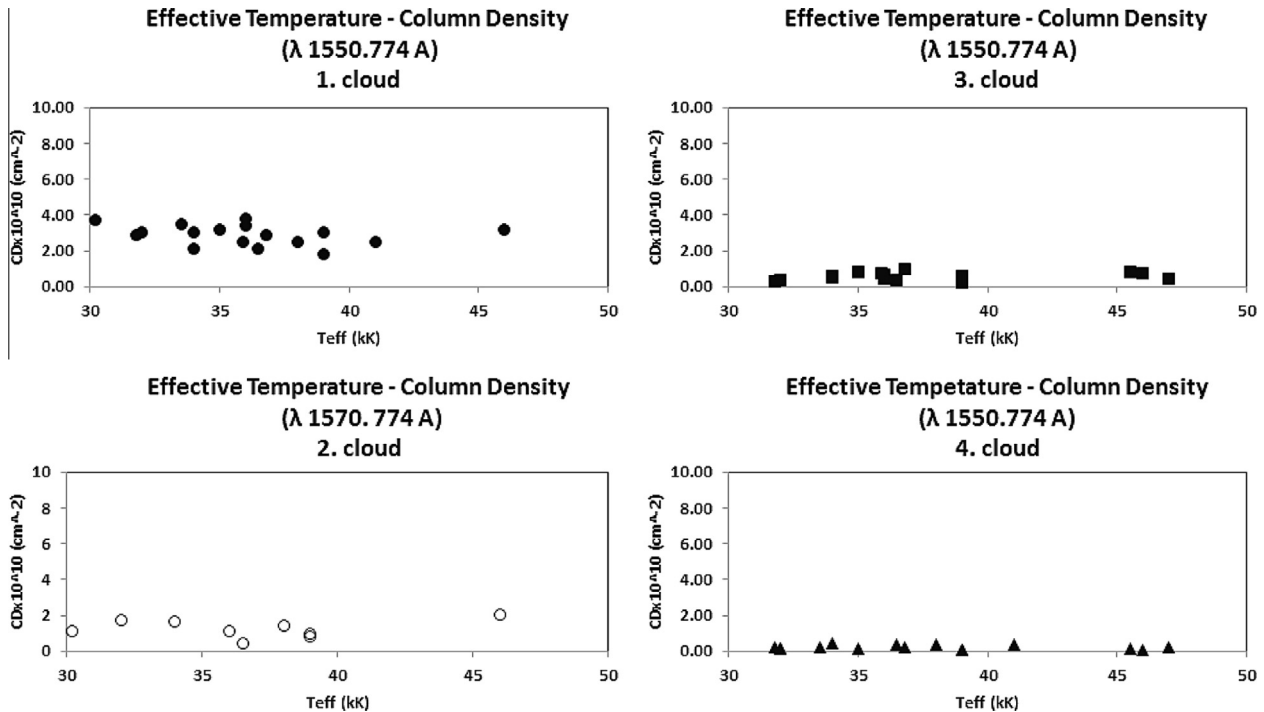


Fig. 14. The variation of the column density (CD) of the C IV resonance line  $\lambda$  1550.774 Å, for the independent density regions of matter, which create the absorption components, as a function of the effective temperature.

below. The first group has an average value of about 1438 km/s, the second group has an average value of about 608 km/s, the third group has an average value of about 243 km/s and the fourth one of about 69 km/s. We remind that the high values of the rotational velocities have to do with the environment of hot emission stars, where, apart from the density regions, the violent mass ejection may produce smaller regions due to micro-turbulent movements. These smaller regions produce narrow absorption components with different shifts that create a sequence of lines. The addition of all the lines of this sequence gives us the sense of line broadening. We also mentioned, as another possible explanation, the division of a spectral line which corresponds to not acceptable rotational velocities in two or more components with lower rotational velocities.

#### Radial velocities

The variation of the radial velocities, as a function of the studied stars' effective temperature of the clouds, which create the C IV resonance lines ( $\lambda\lambda$  1548.155, 1550.774 Å), present a slightly negative slope for the 1st and 2nd cloud and an almost constant behavior for the 3rd and 4th cloud. The negative slope corresponds to high values of radial velocities (between 2000 and 3000 km/s). These high values indicate, eruptive phenomena in some of the studied stars. We also calculated a "good" correlation for the three components ( $R^2 = 0.6132, 0.6, 0.5124$ ) and "weak" linear correlation for the 4th one ( $R^2 = 0.3222$ ).

#### Random velocities

The variation of the random velocities of the ions of the C IV resonance lines ( $\lambda\lambda$  1548.155, 1550.774 Å) for the

independent density regions of matter which create the absorption components, as a function of the effective temperature, presents an almost constant trend with values between 120 until 200 km/s for the first three clouds and about 80 km/s for the fourth one. The linear correlation is "good".

#### Full Width at Half Maximum (FWHM)

The variation of the FWHM is the same as the variation of the rotational and random velocities. This is expected because the FWHM is a parameter which indicates the line broadening and the rotational and random velocities are parameters which contribute to this situation. The average values of the FWHM are 13.0, 6.6, 2.2 and 1.1 Å, respectively.

#### Optical depth, absorbed energy

These parameters have the same slope and the same behavior. This is in agreement with the atomic theory.

#### Column density

The variation of the column density of the C IV resonance lines ( $\lambda\lambda$  1548.155, 1550.774 Å) remains almost constant between  $1 \times 10^{10}$  and  $4 \times 10^{10} \text{ cm}^{-2}$ .

Finally, we note that we found a good correlation between the stars' effective temperature and the radial and random velocities. The same phenomenon has been detected in the case of the Be stars Antoniou et al. (2011) and Antoniou et al. (2012). This means that in Oe and Be stars, if we know the star's effective temperature, we could estimate the above mentioned parameters. However, this must be confirmed by a greater sample of Oe and Be stars and it is a part of our future work.

### Acknowledgements

This research project is in progress at the University of Athens, Department of Astrophysics, Astronomy and Mechanics; we are thankful to the Special Account for Research Grants for the financial support. This work was also supported by the Ministry of Science and Technological Development of Serbia through the projects “Influence of collisional processes on astrophysical plasma line shapes” and “Astrophysical spectroscopy of extragalactic objects”. We also acknowledge the use of the data from SDSS DR7 survey.

### Appendix A. Method of analysis. The Gauss-Rotation model (GR model)

In the context of GR Model, the radiative transfer equation for a complex atmosphere has been solved. By solving the equation (Danezis et al., 2003; Danezis et al., 2007), we calculated the final line function that can fit not only each one of the spectral lines (emission or absorption) but all the complex spectral regions of an ion line

$$I_\lambda = [I_{\lambda_0} \prod_i \exp(-L_i \xi) + \sum_j S_{\lambda_{ej}} (1 - \exp(L_{ej} \xi_{ej})) \prod_g \exp(L_g \xi_g)]$$

where  $\lambda_0$  is the initial radiation intensity,  $L_i, L_{ej}, L_g$  are the distribution functions of the absorption coefficients,  $k_{\lambda_i}, k_{\lambda_{ej}}, k_{\lambda_g}, \xi$  is the optical depth in the center of the spectral line,  $S_{\lambda_{ej}}$  is the source function, that is constant during one observation.

As one can see in the final line function, in the case of a group of absorption lines, the derived complex spectral line profile is described by a new function which is not the superposition of absorption components but the mathematical product of them ( $\prod_{i=1}^N f_i$ ). This means that the final complex profile is not the summation of different functions ( $\sum_{i=1}^N f_i$ ) but the mathematical product of them. Each individual function describes the absorption component of each cloud. The product of a series of functions ( $\prod_{i=1}^N f_i$ ) is a new function and has nothing to do with the sum of functions ( $\sum_{i=1}^N f_i$ ). In contrary, in the case of a group of emission spectral lines the derived complex spectral line profile is described by the summation of different functions ( $\sum_{i=1}^N f_i$ ) and not the product ( $\prod_{i=1}^N f_i$ ).

The GR Model includes the creation of two new distributions, the Rotation distribution (Danezis et al., 2003; Lyratzi et al., 2007) that describes the rotation of the plasma clouds and the Gauss-Rotation distribution (Danezis et al., 2007; Danezis et al., 2009), which describes the combination of the random motions of the clouds’ ions and the self-rotation of the clouds.

The Rotation distribution is

$$L(\lambda) = \sqrt{1 - \cos^2 \theta_0}$$

if

$$\cos \theta_0 = \frac{-\lambda_0 + \sqrt{\lambda_0^2 + 4\Delta\lambda_{rotation}^2}}{2\Delta\lambda_{rotation}z_0} < 1$$

and

$$L(\lambda) = 0$$

if

$$\cos \theta_0 = \frac{-\lambda_0 + \sqrt{\lambda_0^2 + 4\Delta\lambda_{rotation}^2}}{2\Delta\lambda_{rotation}z_0} \geq 1$$

The Gauss-Rotation distribution is

$$L_{final}(\lambda) = \frac{\sqrt{\pi}}{2\lambda_0 z} \int_{-\frac{\pi}{2}}^{\frac{\pi}{2}} \left[ \operatorname{erf} \left( \frac{\lambda - \lambda_0}{\sigma\sqrt{2}} + \frac{\lambda_0 z}{\sigma\sqrt{2}} \cos \theta \right) - \operatorname{erf} \left( \frac{\lambda - \lambda_0}{\sigma\sqrt{2}} - \frac{\lambda_0 z}{\sigma\sqrt{2}} \cos \theta \right) \right] \cos \theta d\theta$$

where  $\operatorname{erf}(x) = \frac{2}{\pi} \int_0^x e^{-u^2} du$ ,  $\lambda_0 = \lambda_{lab} \pm \Delta\lambda_{rot}$ ,  $z = \frac{V_{rot}}{c}$  and  $\sigma$  is the Gaussian typical deviation.

In the line function the factors  $e^{-L_i \xi_i}$  and  $S_{\lambda_{ej}}(1 - e^{L_{ej} \xi_{ej}})$  are the distribution functions of the absorption and the emission component, respectively. The factor  $L$  must include the geometry and all the principle physical conditions of the region that produces the spectral line. This means that if we choose the right physical conditions in the calculations of the factor  $L$ , the factors  $e^{-L_i \xi_i}$  and  $S_{\lambda_{ej}}(1 - e^{L_{ej} \xi_{ej}})$  take the form of a Gauss, Lorentz, Voigt, Rotation or Gauss-Rotation distribution function. In this case we do not use the pure mathematical distributions that do not include any physical parameter, but the physical expression of these distributions. In the case of Gaussian-Rotation model for the classical distributions we use the following physical expressions.

For the Gauss distribution,  $L$  takes the form

$$L_G = e^{-\frac{(\lambda - \lambda_0)^2}{2\sigma^2}}$$

For the Lorentz distribution,  $L$  takes the form

$$L_L = \frac{1}{1 + \left(\frac{\lambda - \lambda_0}{\gamma}\right)^2}$$

For the Voigt distribution,  $L$  takes the form

$$L_V = \int_{-\infty}^{\infty} \frac{e^{-\frac{(\lambda' - \lambda_0)^2}{2\sigma^2}}}{1 + \left(\frac{\lambda - \lambda'}{\gamma}\right)^2} d\lambda'$$

As we mentioned, using the GR model we can calculate some important parameters of the plasma clouds that construct the components of the observed spectral feature. Directly we calculate the apparent rotational ( $V_{rot}$ ) and radial ( $V_{rad}$ ) velocities of absorbing or emitting density

clouds, the Gaussian typical deviation of the ions' random motions ( $\sigma$ ) and the optical depth in the center of the absorption or emission components ( $\xi_i$ ). Indirectly we can calculate, the random velocities of the ions ( $V_{rand}$ ), the ( $FWHM$ ), the absorbed or emitted energy ( $E_a, E_e$ ) and the column density ( $CD$ ).

## Appendix B. Some notes about the linear regression and the linear correlation coefficient

Suppose there are  $n$  data points  $(y_i, x_i)$ , where  $i = 1, 2, \dots, n$ . The goal is to find the equation of the straight line  $y = \alpha + \beta x$  which would provide a “best” fit for the data points. Here the “best” will be understood as in the least-squares approach: such a line that minimizes the sum of squared residuals of the linear regression model. In other words, numbers  $\alpha$  (the  $y$ -intercept) and  $\beta$  (the slope) solve the following minimization problem:

Find  $\min Q(\alpha, \beta)$  where

$$Q(\alpha, \beta) = \sum_{i=1}^n \hat{\epsilon}_i^2 = \sum_{i=1}^n (y_i - \alpha - \beta x_i)^2$$

Solving the above minimization problem we take the equation of the asked straight line:

$$\hat{y} = \hat{\alpha} + \hat{\beta}x$$

where

$$\hat{b} = \frac{\sum x_i y_i - (\sum x_i)(\sum y_i)}{n \sum x_i^2 - (\sum x_i)^2} \quad \text{and} \quad \hat{\alpha} = \bar{y} - \hat{\beta}x$$

The linear correlation coefficient  $R$  between  $y$  and  $x$  is calculated by

$$R = \frac{\sum (x_i - \bar{x})(y_i - \bar{y})}{\sqrt{\sum (x_i - \bar{x})^2} \sqrt{\sum (y_i - \bar{y})^2}}$$

With regard to the linear correlation coefficient  $R^2$  we note that if  $R^2 = 1$  the linear correlation between  $y$  and  $x$  is considered as “ideal”, if  $0.5 < R^2 < 1$  the linear correlation is

considered as “good” and if  $0.3 < R^2 < 0.5$  the linear correlation is considered as “weak”. Otherwise there is no linear correlation. For more details see (e.g. Kleinbaum et al., 1987 Ch. 5,6)

## References

- Antoniu, A., Danezis, E., Lyrtzi, E., Nikolaidis, D., Popovic, L.C., Dimitrijevic, M.S., 2007. A statistical study of physical parameters of the C IV density regions in 20 Oe stars. Spectral Lines Shapes in Astrophysics, VI Serbian Conference (VI SCSLSA). AIP Conf. Proc., 936.
- Antoniu, A., Danezis, E., Lyrtzi, E., Stathopoulos, D., Dimitrijevic, M.S., 2011. A statistical study of the Si IV resonance line parameters in 19 Be stars. Baltic Astron. 20, 548–551.
- Antoniu, A., Danezis, E., Lyrtzi, E., Stathopoulos, D., 2012. The structure of the Si IV region in Be stars: a study of Si IV spectral lines in 68 Be stars. J. Phys. Conf. Ser. 399, 012021.
- Bates, B., Halliwell, D.R., 1986. Discrete absorption components in spectra of mass-losing stars – an analytical model for the trajectories of gas parcels and streams. MNRAS 223, 673–681.
- Danezis, E., Theodossiou, E., Laskarides, P.G., 1991. The far UV spectrum of the Be star AX Monocerotis. Ap&SS 179, 111–139.
- Danezis, E., Lyrtzi, E., Stathopoulos, M., Theodossiou, E., Nikolaidis, D., Drakopoulos, C., Soulikias, A., Antoniu, A., 2003. On modeling SACs regions in early type atmospheres. Publ. Astron. Obs. Belgrade 76, 179–183.
- Danezis, E., Nikolaidis, D., Lyrtzi, E., Popović, L.Č., Dimitrijević, M.S., Antoniu, A., Theodosiou, E., 2007. A new model for the structure of the DACs and SACs regions in the Oe and Be stellar atmospheres. PASJ 59, 827–834.
- Danezis, E., Lyrtzi, E., Popović, L.Č., Dimitrijević, M.S., Antoniu, A., 2009. Interpreting the complex line profiles in the stellar spectra. New Astron. Rev. 53, 214–221.
- Doazan, V., Sedmak, G., Barylak, M., Rusconi, L., 1991. A Be Star Atlas of Far UV and Optical High Resolution Spectra, ESA SP-1147. ESA Sci. Publ, Paris.
- Kleinbaum, D.G., Kupper, L.L., Muller, K.E., 1987. Applied Regression Analysis and Other Multivariate Methods, 2nd edition. PWS-Kent Publishing Company, Boston.
- Lyrtzi, E., Danezis, E., Popović, L.Č., Dimitrijević, M.S., Nikolaidis, D., Antoniu, A., 2007. The Complex Structure of the MgII  $\lambda\lambda$  2795.523, 2802.698 ARegions of 64 Be Stars. PASJ 59, 357–371.
- Snedecor, G.W., Cochran, W.G., 1989. Statistical Methods, 8th edition. Iowa State University Press, Ames, IA.